Inter*net* Electronic Journal of Molecular Design

August 2004, Volume 3, Number 8, Pages 464–473

Editor: Ovidiu Ivanciuc

Proceedings of the Internet Electronic Conference of Molecular Design, IECMD 2003
November 23 – December 6, 2003
Part 2

On the Existence of the Butterfly Isomer of Al_2H_2: *Ab Initio* Coupled–Cluster Study

Jerzy Moc and Maria Wierzejewska

Faculty of Chemistry, Wroclaw University, F. Joliot–Curie 14, 50–383 Wroclaw, Poland

Received: October 31, 2003; Revised: April 22, 2004; Accepted: May 1, 2004; Published: August 31, 2004

Citation of the article:
J. Moc and M. Wierzejewska, On the Existence of the Butterfly Isomer of Al_2H_2: *Ab Initio* Coupled–Cluster Study, *Internet Electron. J. Mol. Des.* **2004**, *3*, 464–473, http://www.biochempress.com.

Inter*net* Electronic Journal of Molecular Design

BioChem Press
http://www.biochempress.com

On the Existence of the Butterfly Isomer of Al_2H_2: *Ab Initio* Coupled–Cluster Study[#]

Jerzy Moc* and Maria Wierzejewska

Faculty of Chemistry, Wroclaw University, F. Joliot–Curie 14, 50–383 Wroclaw, Poland

Received: October 31, 2003; Revised: April 22, 2004; Accepted: May 1, 2004; Published: August 31, 2004

Internet Electron. J. Mol. Des. **2004**, *3* (8), 464–473

Abstract

Motivation. The recent theoretical study of the present authors revealed that the butterfly structure of Ga_2H_2 subhydride was an additional dibridged minimum on the singlet potential energy surface. Here, the existence of this kind of isomer is studied for the lighter Al_2H_2 analog in terms of thermodynamic and kinetic stabilities using high level *ab initio* calculations.

Method. Geometry optimization of the key dibridged structures were performed using *ab initio* coupled–cluster singles and doubles method incorporating a perturbative correction for triples (CCSD(T)) with all the electrons correlated (FU) and in conjunction with the aug–cc–pVTZ basis set. Better energetics were evaluated at the CCSD(T)(FU) level and employing aug–cc–pVrZ (r = Q, 5Z) basis sets.

Results. The calculated thermodynamic and kinetic stabilities and IR spectra of the five Al_2H_2 structural isomers **1**–**5**, including a new type nonplanar dibridged (butterfly) species **5** not reported before, have been compared.

Conclusions. The butterfly isomer **5** has been found to be the lowest energy structure of Al_2H_2, although lying only about 1 kcal/mol below the "previously most preferred" planar dibridged isomer **1** at the ZPE corrected CCSD(T)(FU)/aug–cc–pV5Z computational level.

Keywords. Aluminum subhydride Al_2H_2; three bridged and two non–bridged isomers; isomerization mechanisms; kinetic stabilities; vibrational frequencies and IR intensities.

Abbreviations and notations

Aug–cc–pVrZ, Augmented correlation–consistent polarized valence r–zeta (r = T (triple), Q (quadruple), 5Z (quintuple)	CCSD(T), CCSD with a perturbative correction for triples
CCSD, Coupled–cluster singles and doubles	PES, Potential energy surface
	TS, Transition state
	ZPE, Zero point energy

1 INTRODUCTION

Simple binary hydrides still present a challenge for synthetic chemists as exemplified by hydride compounds containing the Group 13 atoms [1]. There is a dramatic difference between the hydride chemistry of boron with a large number of boron hydrides identified and characterized and the hydride chemistry of its heavier congeners for which only a few binary hydrides are known [1–3].

[#] Presented in part at the Internet Electronic Conference of Molecular Design, IECMD 2003.

* Correspondence author; phone: 48–71–375–7267; fax: 48–71–222–348; E–mail: jmoc@wchuwr.chem.uni.wroc.pl.

For instance, the recent matrix isolation infrared (IR) studies of Downs *et al*. have shown that the dibridged $M(\mu–H)_2M$ species are formed in low temperature argon matrices for M = Ga and In [4,5]. Interestingly, these species have been found to photoisomerize to the other M_2H_2 (M = Ga, In) structures [4,5]. As far as the binary aluminum hydrides are concerned, the recent IR identification of Al_2H_4 and Al_2H_6 compounds in solid hydrogen as reported by Andrews and co–workers is an important contribution in the field [2,6]. These authors studied the reaction of laser–ablated Al atoms with pure H_2 during codeposition at 3.5 K followed by UV photolysis at 6.5 K and isotopic substitution with the aim to isolate and assign the target hydride compounds. The other binary hydrides of aluminum, including dialuminum subhydride Al_2H_2, were also detected in these experiments [6]. The first experimental evidence of the presence of Al_2H_2 isomers came from the IR spectra of the matrices containing the products of reactions of laser–ablated Al atoms with H_2 in excess argon by Chertihin and Andrews [7]. In addition to the major reaction products, AlH, AlH_2 and AlH_3, the distinct Al_2H_2 species were also observed. With the help of the subsequent high level *ab initio* calculations [8] it was concluded that the Al_2H_2 species detected in solid Ar [7] were the planar dibridged $Al(\mu–H)_2Al$ and monobridged $HAl(\mu–H)Al$ isomers.

Computationally, dialuminum subhydride Al_2H_2 has been studied by using *ab initio* [8–11] and DFT [12] quantum mechanical methods. In 1985 Baird [9] performed SCF and MP2 calculations with modest size basis sets for the singlet planar dibridged $Al(\mu–H)_2Al$, branched $AlAlH_2$ and trans–bent HAlAlH structures. More recently, Schaefer and co–workers [8,10] employed SCF, single and double excitation configuration interaction (CISD) and coupled cluster (CCSD and CCSD(T)) methods in conjunction with double–zeta plus polarization (DZP) and triple–zeta plus single and double polarization (TZP, TZ2P) plus f functions on Al basis sets in the latter case (TZ2Pf). They calculated structures, relative energies and vibrational frequencies of the four Al_2H_2 singlet isomers: planar dibridged $Al(\mu–H)_2Al$ (D_{2h}) **1**, branched $AlAlH_2$ (C_{2v}) **2**, trans–bent HAlAlH (C_{2h}) **3** and planar monobridged $HAl(\mu–H)Al$ (C_s) **4**. By using effective–core potential (ECP) on heavy atoms and valence DZP basis sets, Treboux and Barthelat [11] performed SCF and CI calculations of the **1**–**4** isomer types for the X_2H_2 series with X belonging to Group 13. Jursic [12] carried out DFT calculations using B3LYP, BLYP and SVWN functionals and the 6–311G(2d,2p) basis set to assess the quality of the DFT predictions for relative stabilities and frequencies of the **1**–**4** Al_2H_2 isomers. To aid in experimentally characterizing Al_2H_2, Chertihin and Andrews [7] performed many–body perturbation theory (MBPT(2)) calculations with DZP basis set for the singlet **1**, **3**, **4** and triplet **1**, **3** Al_2H_2 isomers including partially and fully deuterated forms. All the previous computational studies of Al_2H_2 [8–12] found consistently the singlet planar dibridged $Al(\mu–H)_2Al$ species **1** to be of the lowest energy.

Apparently, an experimental detection of the nonplanar dibridged (butterfly) isomer of Al_2H_2, designated here as the structural type **5**, has not been reported. Similarly, the butterfly structure has not been located in the previous computational studies of Al_2H_2 [8–12]. By contrast, this kind of structure corresponds to the minimum on the potential energy surface (PES) of the X_2H_2 hydrides with X belonging to Group 14 [13–17] and it was actually detected and characterized in the gas phase for X = Si [18] and in the solid matrices for X = Si, Ge and Sn [16,17,19]. Furthermore, we located recently the butterfly minimum on the singlet PES of Ga_2H_2 using the correlated *ab initio* and DFT methods and large 6–311++G(3df,3pd) basis set [20]. The present results for Al_2H_2 show that the butterfly isomer **5** is the lowest energy structure, lying however only about 1 kcal/mol below the planar dibridged structure **1** at our best computational level. Another issue addressed for the first time in this work is that of kinetic stability of all the Al_2H_2 singlet isomers.

2 COMPUTATIONAL METHODS

Optimized structures and corresponding energy second derivatives with respect to the nuclear coordinates (hessians) were found to provide harmonic vibrational frequencies and zero–point energy (ZPE) corrections. The aug–cc–pVTZ (augmented correlation–consistent polarized valence triple–zeta) basis set [21–23] was used for this purpose. The structures and Hessians were calculated with second–order Møller–Plesset perturbation theory (MP2) [24] that correlates all electrons (technically designated FULL, abbreviated FU) and, for both dibridged isomers, with coupled–cluster singles and doubles method including a perturbative estimate of triples (CCSD(T)(FU)) [25]. The latter calculations have been performed numerically. Minima were connected to each transition state (TS) by tracing the MP2(FU) intrinsic reaction coordinate (IRC) [26]. The CCSD(T)(FU) energy calculations at the MP2(FU) structures using the aug–cc–pVrZ basis sets with r =T, Q [21–23] were performed next. For the thermodynamically most stable dibridged structures **1** and **5**, the aug–cc–pV5Z basis [21–23] was also employed in the CCSD(T)(FU) calculations. The Gaussian 98 code was used throughout [27].

3 RESULTS AND DISCUSSION

In Figure 1, the MP2(FU) and CCSD(T)(FU) structures of the **1**–**5** isomers of Al_2H_2 and the located isomerization transition states are displayed, and in Figure 2 the potential energy diagram for the singlet Al_2H_2 is shown. The relative energies of all the species calculated at CCSD(T)(FU) using aug–cc–pVrZ (r = T, Q) basis sets at the MP2(FU) geometries are presented in Table 1. For both dibridged isomers **1** and **5** and transition state linking them **TS1–5**, Table 1 also contains the CCSD(T)(FU) results obtained with the larger aug–cc–pV5Z basis. In the next sections, the ZPE corrected CCSD(T)(FU)/aug–cc–pVQZ relative energies will be used for the purpose of discussion, unless otherwise indicated.

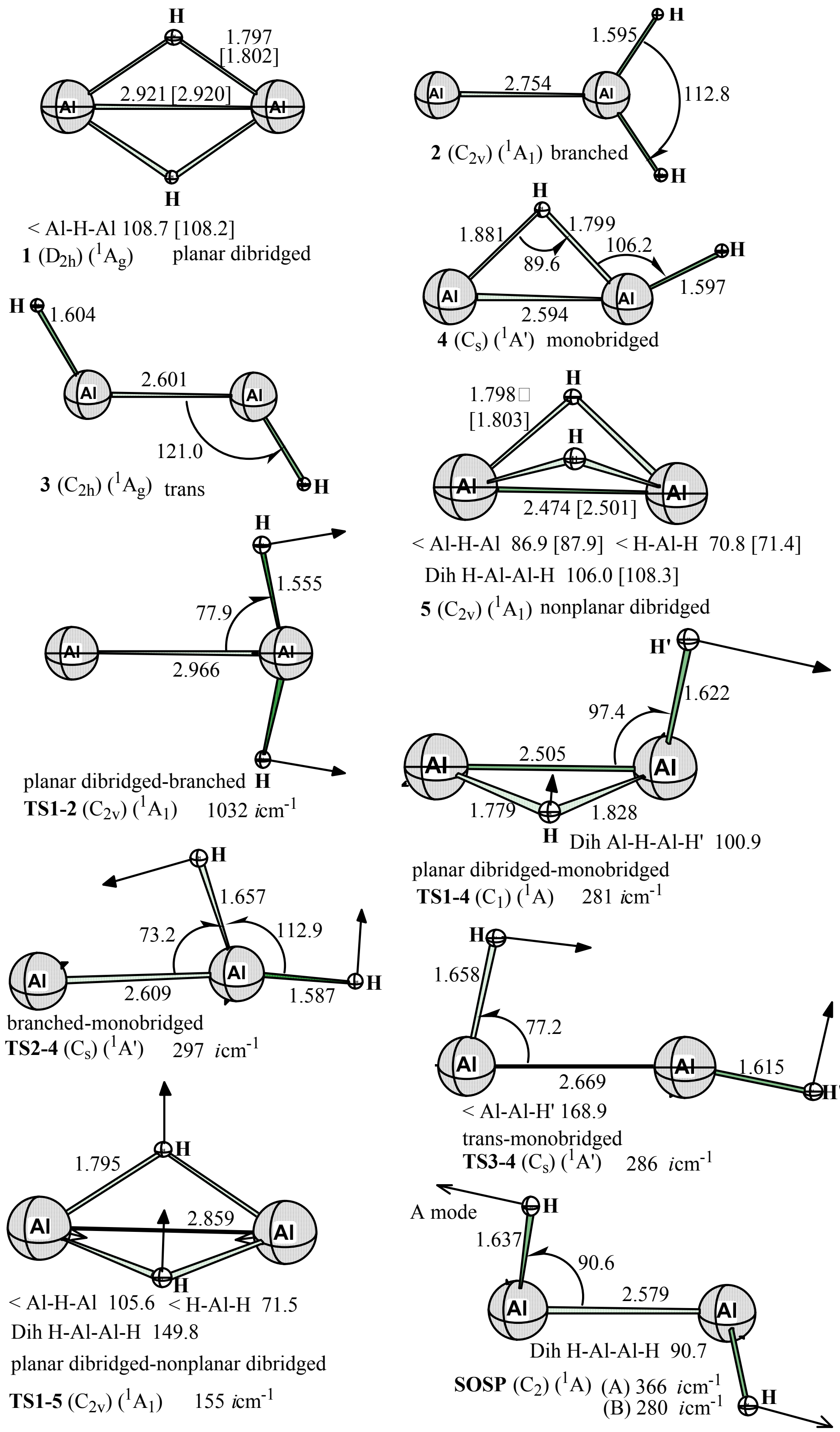

Figure 1. Minima and transition states found on the singlet potential energy surface of Al_2H_2 using MP2(FU) and CCSD(T)(FU) methods in conjunction with the aug–cc–pVTZ basis set (bond lengths in angstroms, bond angles in degrees); the reaction coordinate vector and the corresponding imaginary frequency are included for each transition state and, for **SOSP** (second–order saddle point), the A imaginary mode is shown together with both A and B imaginary frequencies. CCSD(T)(FU) results are given in square brackets.

3.1 Bridged vs. Non–bridged Type Isomers

Previously, only the Al_2H_2 isomers **1–4** were treated computationally [8–12]. Our optimized structures of these isomers are in agreement with the earlier results. The reported high level ZPE corrected CCSD(T) results obtained using large atomic natural orbital (ANO) basis set within the frozen–core approximation (the values denoted by Schaefer et al as "best" in Ref. [10]) place the energies of **2**, **3**, **4** at 7.6, 13.5 and 8.5 kcal/mol relative to **1**. This can be compared with our CCSD(T)(FU) assessment of 9.4, 14.6 and 9.1 kcal/mol, respectively. In both cases a tight stability competition is predicted between the branched $AlAlH_2$ (C_{2v}) **2** and monobridged HAl(μ–H)Al (C_s) **4**. The findings of Schaefer [10] indicate the isomer **2** to be more stable than **4** by 0.9 kcal/mol, whereas our results favor the isomer **4** over **2** by 0.3 kcal/mol. The two CCSD(T) calculations agree that all the structures lie within a narrow energy interval of 13.5 (Schaefer) and 14.6 (this work) kcal/mol. On the basis of CCSD(T)/TZ2Pf frequency calculations [8] complementing the earlier matrix isolation IR study of Chertihin and Andrews it was concluded that the Al_2H_2 species actually detected [7] were the planar dibridged **1** and monobridged **4**.

Table 1. Relative energies (kcal/mol) of the singlet Al_2H_2 isomers and isomerization transition states calculated at the CCSD(T)(FU) level [a]

Species	aug–cc–pVTZ		aug–cc–pVQZ		aug–cc–pV5Z	
	ΔE	ΔE+ΔZPE	ΔE	ΔE+ΔZPE	ΔE	ΔE+ΔZPE
1(D_{2h}) (^1A_g)	1.4 (1.4)[b]	0.7 (0.7)[b,c]	2.3 (2.2)[b]	1.5 (1.5)[b,c]	1.7 (1.7)[b]	0.9 (0.9)[b,c]
2(C_{2v}) ($^1A_1$)	10.4	9.7	11.6	10.9		
3(C_{2h}) (^1A_g)	16.6	15.2	17.6	16.1		
4(C_s) ($^1A'$)	10.6	9.3	11.9	10.6		
5(C_{2v}) ($^1A_1$)	0.0 (0.0)[b]	0.0 (0.0)[b,c]	0.0 (0.0)[b]	0.0 (0.0)[b,c]	0.0 (0.0)[b]	0.0 (0.0)[b,c]
TS1–2(C_{2v}) ($^1A_1$)	53.7	52.6	55.6	54.4		
SOSP(C_2) (^1A)	22.4	19.9	23.1	20.6		
TS1–4(C_1) (^1A)	12.8	11.7	12.8	11.6		
TS1–5(C_{2v}) ($^1A_1$)	1.4	0.7	2.1	1.4	1.6	0.9
TS2–4(C_s) ($^1A'$)	13.9	12.6	14.8	13.4		
TS3–4(C_s) ($^1A'$)	21.0	18.8	22.4	20.2		
2AlH($^1\Sigma^+$)	35.8	32.2	41.4	37.9		

[a] At the MP2(FU)/aug–cc–pVTZ geometries, unless indicated otherwise
[b] At the CCSD(T)(FU)/aug–cc–pVTZ geometry
[c] Result corrected for the unscaled CCSD(T)(FU) ZPE
[d] At 298.15K, the respective ΔH [ΔG] values for **1**, **5**, **TS1–5** are: (r = T) 0.9 [0.7], 0.0 [0.0], 0.5 [0.8], (r = Q) 1.8 [1.6], 0.0 [0.0], 1.2 [1.5], (r = 5Z) 1.2 [1.0], 0.0 [0.0], 0.7 [0.9] kcal/mol

Consistent with the recent finding for the Ga_2H_2 congener [20], an additional dibridged minimum **5** corresponding to the non–planar C_{2v} structure has been located on the singlet PES of Al_2H_2. Using the aug–cc–pVTZ basis set, the butterfly minimum was first found at MP2(FU) and the viability of this stationary point was substantiated with the follow–up geometry optimization and frequency calculation at the CCSD(T)(FU) level (Figure 1). As seen previously for Ga_2H_2 [20], **5** exhibits a relatively short Al–Al distance of 2.474 and 2.501 Å at MP2(FU) and CCSD(T)(FU), respectively, with the HAlAlH dihedral angle of 106.0 and 108.3°. Also, similar to Ga_2H_2, the two dibridged Al_2H_2 structures **1** and **5** are found to be very close in terms of thermodynamic stability, with an energy separation of only 2.3 (1.5) kcal/mol at the CCSD(T)(FU)/aug–cc–pVQZ (+ZPE) level. This energy difference decreases to 1.7 (0.9) kcal/mol when the augmented valence quintuple–zeta quality aug–cc–pV5Z basis set is used. However, unlike the Ga_2H_2 case, this is the isomer **5** which is predicted to be the more stable structure (Table 1).

To examine the effect of the optimized geometry on the stability order of the two dibridged isomers, further CCSD(T)(FU) calculations using the aug–cc–pVrZ basis sets (r = Q, 5Z) were also performed at the CCSD(T)(FU)/aug–cc–pVTZ optimized structures (cf. the values in parentheses in Table 1). It is seen that the latter calculations changed neither the energy separation obtained with each basis set at the MP2(FU) optimized structures nor the preference for the butterfly form. Note that in the next section we also discuss the influence of the thermal correction (T = 298.15 K) on the relative stability of **1** and **5** (as suggested by the reviewer) and the issue of the kinetic stability of the two species.

3.2 Rearrangement Paths and Kinetic Stabilities

The PES profile for the interconversion of the **1**–**5** singlet Al_2H_2 isomers (Figure 2) parallels that found previously for Ga_2H_2 [20]. There is also a large degree of resemblance between the corresponding isomerization transition state structures of the two molecular systems. Therefore, we shall summarize the Al_2H_2 results only briefly with the underlining distinct features revealed in this work. (*i*) The planar dibridged isomer **1** rearranges preferably to the branched **2** or trans **3** species via a two–step mechanism with the monobridged isomer **4** serving as the intermediate. Both paths can be written as follows: **1** $\rightarrow$ **TS1–4** $\rightarrow$ **4** $\rightarrow$ **TS2–4** $\rightarrow$ **2** and **1** $\rightarrow$ **TS1–4** $\rightarrow$ **4** $\rightarrow$ **TS3–4** $\rightarrow$ **3**, respectively, where the single hydrogen bridge is broken in each reaction step. (*ii*) The rearrangement of the branched species **2** into trans **3** can also be accomplished in two steps if one follows the path: **2** $\rightarrow$ **TS2–4** $\rightarrow$ **4** $\rightarrow$ **TS3–4** $\rightarrow$ **3**. (*iii*) The transition states involved in the two–step mechanisms are found to lie about 10–19 kcal/mol above **1**. (*iv*) The highest calculated isomerization barrier (53 kcal/mol) is for the one step rearrangement of **1** into **2** via **TS1–2**. However, these results should be seen together with the calculated kinetic stability of **1** discussed below.

The planar **1** and nonplanar **5** dibridged minima are connected through the **TS1–5** transition state (note that we have not pursued **TS1–5** at CCSD(T)(FU)). The imaginary mode of **TS1–5** corresponds to the butterfly motion of the hydrogens combined with the Al–Al stretching (Figure 1). The calculated CCSD(T)(FU)/aug–cc–pVrZ barrier separating the lowest energy isomer **5** from the second lowest isomer **1** (**5** $\rightarrow$ **1** rearrangement) is found to be 1.4, 2.1 and 1.6 kcal/mol for r =T, Q and 5Z, respectively. After the inclusion of ZPE, this barrier decreases to 0.7, 1.4 and 0.9 kcal/mol (Table 1). For the reverse isomerization **1** $\rightarrow$ **5**, the calculated barrier is not existent being 0.0, –0.2, –0.1 kcal/mol for r = T, Q and 5Z, respectively, and 0.0, –0.1 and 0.0 kcal/mol when the

ZPE correction is included. These results indicate that in the gas phase the isomer **1** rearranges to **5** with no barrier. Apparently, the PES of Al_2H_2 is quite flat along the butterfly mode: the decrease of the H–Al–Al–H dihedral angle from 180.0° (**1**) to 149.8° (**TS1–5**) to 106.0° (**5**) is accompanied by the energy change of *ca*. 1 kcal/mol at the ZPE corrected CCSD(T)(FU)/aug–cc–pV5Z level (Table 1). An additional check of the relative stability of **1** and **5** is based on the enthalpy (ΔH) and Gibbs free energy (ΔG) values, the latter two calculated at T = 298.15 K (p = 1atm) using vibrational frequencies evaluated at MP2(FU) (see footnote d) under Table 1). The respective ΔH [ΔG] values for **1** and **5** are found to be 0.9 [0.7] and 0.0 [0.0] (r = T), 1.8 [1.6] and 0.0 [0.0] (r = Q), and 1.2 [1.0] and 0.0 [0.0] (r = 5Z) kcal/mol. In terms of ΔH [ΔG], the barrier separating **5** from **1** (**5** →**TS1–5** →**1**) is calculated to be 0.5 [0.8], 1.2 [1.5] and 0.7 [0.9] kcal/mol for r = T, Q and 5Z, respectively. Again, for the reverse (**1** → **5**) barrier disappears as the calculated ΔH [ΔG] are –0.4 [0.1], –0.6 [–0.1] and –0.5 [–0.1] kcal/mol for r = T, Q and 5Z. These results support the stability predictions discussed in the previous section.

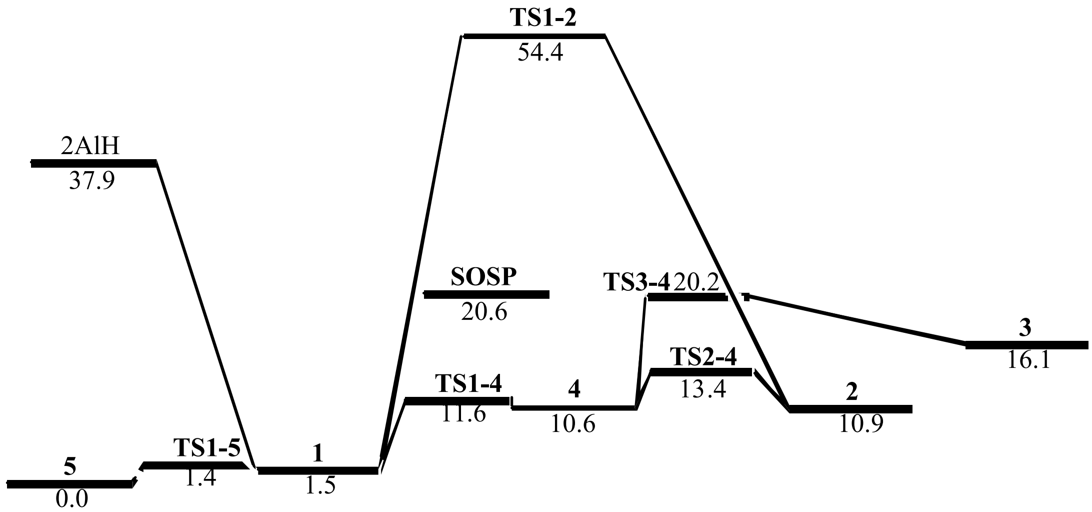

Figure 2. The potential energy diagram for the singlet Al_2H_2 calculated at the CCSD(T)(FU)/aug–cc–pVQZ + ZPE level. All energies are in kcal/mol.

3.3 Vibrational Frequencies and IR Intensities

Table 2 summarizes the vibrational frequencies and IR intensities calculated here at MP2(FU) and CCSD(T)(FU) for the **1**–**5** singlet Al_2H_2 isomers and those reported from the argon matrix experiment [7]. For comparison, the previous CCSD(T) results [8,10] are also included. Consistent with the earlier experience [8,10], the experimental frequencies of Al_2H_2 are rather poorly reproduced with the large basis set correlated *ab initio* calculations unless a proper scaling factor is used [8]. One reason of this discrepancy is of course the anharmonicity of the modes involved. On the other hand, one notices a good correlation between the predicted infrared intensities and the presence of the corresponding bands for the **1**, **3** and **4** species [7,8]. Indeed, the only absorptions detected [7] were those with the highest calculated intensity unless they were beyond the range of the detector used.

Table 2. Comparison of IR spectra calculated and observed for Al_2H_2 isomers [a]

Isomer	Calculations			Ar matrix[d]	Assignment
	MP2(FU)[b]	CCSD(T)(FU)[b]	CCSD(T)[c]		
1	1411 (0)	1384	1384 (0)		$\nu_1(a_g)$
	1312 (2363)	1295	1272 (2182)	1160.9	$\nu_4(b_{1u})$
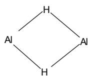	1213 (0)	1184	1128 (0)		$\nu_3(b_{3g})$
	1016 (94)	1003	1007 (109)	844	$\nu_5(b_{2u})$
	334 (0)	330	326 (0)		$\nu_2(a_g)$
D_{2h}	166 (206)	138	137 (165)		$\nu_6(b_{3u})$
2	1881 (339)		1862 (298)		$\nu_5(b_2)$
	1877 (429)		1853 (373)		$\nu_1(a_1)$
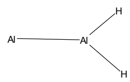	793 (497)		795 (455)		$\nu_2(a_1)$
	416 (159)		390 (150)		$\nu_4(b_1)$
	297 (33)		291 (28)		$\nu_3(a_1)$
C_{2v}	205 (47)		249 (39)		$\nu_6(b_2)$
3	1847 (865)		1806 (870)	1646.9	$\nu_5(b_u)$
	1842 (0)		1802 (0)		$\nu_1(a_g)$
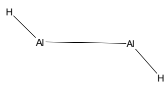	507 (0)		510 (0)		$\nu_2(a_g)$
	288 (0)		246 (0)		$\nu_3(a_g)$
	237 (62)		251 (45)		$\nu_6(b_u)$
C_{2h}	243 (41)		208 (30)		$\nu_4(a_u)$
	1872 (599)		1823 (501)	1668.7	$\nu_1(a')$
4	1262 (297)		1213 (311)	1127	$\nu_2(a')$
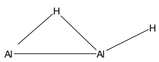	982 (548)		1009 (508)	890	$\nu_3(a')$
	426 (21)		430 (17)		$\nu_4(a')$
C_s	287 (27)		276 (25)		$\nu_5(a')$
	225 (34)		124 (29)		$\nu_6(a'')$
	1419 (63)	1395			$\nu_1(a_1)$
5	1288 (319)	1251			$\nu_5(b_1)$
	1108 (565)	1104			$\nu_4(b_2)$
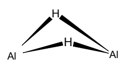	1029 (0)	1018			$\nu_3(a_2)$
C_{2v}	872 (236)	838			$\nu_6(a_1)$
	249 (9)	239			$\nu_2(a_1)$

[a] Frequencies are in cm^{-1}, intensities (in parentheses) in $kcalmol^{-1}$
[b] This work. CCSD(T)(FU) results obtained by numerical second differentiation
[c] For **1**, **2**, **4** from Ref. [8]; CCSD(T)/TZ2Pf results obtained by numerical first differentiation of analytical gradients. For **3**, from Ref. [10]; CCSD/TZ2P results obtained by numerical first differentiation of analytical gradients. The frozen–core (FC) approximation was used in Refs. [8,10]
[d] Data from Ref. [7]

According to the presented interpretation [7,8], the experimental IR spectra gave no evidence for the branched isomer **2** despite the fact that the three modes with the relatively high intensity were found for this species (Table 2). On the basis of the results in Table 2 we suggest that the butterfly species **5**, found here to be the lowest energy isomer, might be present in the low temperature matrices in addition to the other Al_2H_2 species [7,8].

Isomer **5** shows five infrared active modes, three of them being relatively intense, and thus should in principle be observable. Also, a proximity of the calculated frequencies for **5** to the observed features does not allow to exclude the presence of this isomer in the studied matrices [7]. Further experimental work on the possible photo–equilibrium between the different Al_2H_2 species, similar to this reported recently for Ga_2H_2 and In_2H_2 [4,5], might be helpful in clarifying this issue.

4 CONCLUSIONS

In the present contribution we have shown that the non–planar dibridged (butterfly) isomer **5** of Al_2H_2 corresponds to an additional minimum on the singlet PES. Both Al_2H_2 dibridged structures, planar **1** and non–planar **5**, compete to be the lowest energy isomer, with the latter species found to be thermodynamically more stable by *ca*. 1 kcal/mol as based on the ΔE + ΔZPE, ΔH(298.15K) and ΔG(298.15K) results derived from the CCSD(T)(FU) calculations with large aug–cc–pV5Z basis set. The calculated PES of Al_2H_2 is rather flat along the butterfly mode. The revealed isomerization PES profile and transition state structures for the interconversion of the five **1**–**5** Al_2H_2 isomers bear a large resemblance to those found earlier for the gallium analog [20]. The presented *ab initio* results are believed to be useful in further experimental studies aiming at isolation of various Al_2H_2 species.

Acknowledgment

The authors acknowledge a generous support of computing time at the Wroclaw Center for Networking and Supercomputing. J.M. thanks Dr. M. Karni for providing a copy of Ref. [17].

5 REFERENCES

[1] N. W. Mitzel, Molecular Dialane and Other Binary Hydrides, *Angew. Chem. Int. Ed.* **2003**, *42*, 3856–3858.
[2] L. Andrews and X. Wang, The Infrared Spectrum of Al_2H_6 in Solid Hydrogen, *Science* **2003**, *299*, 2049–2052. Erratum, 2 May 2003.
[3] S. Aldridge and A. J. Downs, Hydrides of the Main–Group Metals: New Variations on an Old Theme, *Chem. Rev.* **2001**, *101*, 3305–3365.
[4] H.–J. Himmel, L. Manceron, A. J. Downs and P. Pullumbi, Characterization and Photochemistry of the Gallium and Indium Subhydrides Ga_2H_2 and In_2H_2, *Angew. Chem. Int. Ed.* **2002**, *41*, 796–799.
[5] H.–J. Himmel, L. Manceron, A. J. Downs and P. Pullumbi, Formation and Characterization of the Gallium and Indium Subhydride Molecules Ga_2H_2 and In_2H_2: A Matrix Isolation Study, *J. Am. Chem. Soc.* **2002**, *124*, 4448–4457.
[6] X. Wang, L. Andrews, S. Tam, M. E. DeRose and M. E. Fajardo, Infrared Spectra of Aluminum Hydrides in Solid Hydrogen: Al_2H_4 and Al_2H_6, *J. Am. Chem. Soc.* **2003**, *125*, 9218–9228.
[7] G. V. Chertihin and L. Andrews, Reactions of Pulsed–Laser Ablated Al Atoms with H_2. Infrared Spectra of AlH, AlH_2, AlH_3, and Al_2H_2 Species, *J. Phys. Chem.* **1993**, *97*, 10295–10300.
[8] J. C. Stephens, E. E. Bolton, H. F. Schaefer III and L. Andrews, Quantum Mechanical Frequencies and Matrix Assignments to Al_2H_2, *J. Chem. Phys.* **1997**, *107*, 119–123.
[9] N. C. Baird, Molecular Orbital Calculations for Dialuminum and Disilicon Hydrides and Related Systems, *Can. J. Chem.* **1985**, *63*, 71–76.
[10] Z. Palagyi, R. S. Grev and H. F. Schaefer III, Striking Similarities Between Elementary Silicon and Aluminum Compounds: Monobridged, Dibridged, Trans–Bent, and Vinylidene Isomers of Al_2H_2, *J. Am. Chem. Soc.* **1993**,

115, 1936–1943.
[11] G. Treboux and J.–C. Barthelat, X–X Direct Bonds versus Bridged Structures in Group 13 X_2H_2 Potential Energy Surfaces, *J. Am. Chem. Soc.* **1993**, *115*, 4870–4878.
[12] B. S. Jursic, Structural Properties and Vibrational Spectra of Al_2H_2 Clusters as Evaluated with Density Functional Theory Methods, *J. Mol. Struct.* (*Theochem*) **1998**, *453*, 123–129.
[13] B. T. Colegrove and H. F. Schaefer, Disilyne (Si_2H_2) Revisited, *J. Phys. Chem.* **1990**, *94*, 5593–5602.
[14] Z. Palagy, H. F. Schaefer and E. Kapuy, Ge_2H_2: A Molecule with a Low–Lying Monobridged Equilibrium Geometry, *J. Am. Chem. Soc.* **1993**, *115*, 6901–6903.
[15] S. Nagase, K. Kobayashi and N. Takagi, Triple Bonds Between Heavier Group 14 Elements. A Theoretical Approach, *J. Organomet. Chem.* **2000**, *611*, 264–271.
[16] X. Wang, L. Andrews, G. V. Chertihin and P. F. Souter, Infrared Spectra of the Novel Sn_2H_2 Species and the Reactive $SnH_{1,2,3}$ and $PbH_{1,2,3}$ Intermediates in Solid Neon, Deuterium, and Argon, *J. Phys. Chem. A* **2002**, *106*, 6302–6308.
[17] M. Carni, Y. Apeloig, J. Kapp and P. V. R. Schleyer, Theoretical Aspects of Compounds Containing Si, Ge, Sn and Pb; in: *The Chemistry of Organic Silicon Compounds*, Vol.3, Ed. Z. Rappoport and Y. Apeloig, John Wiley & Sons, 2001, Chapter 1, pp 1–163.
[18] M. Bogey, H. Bolvin, M. Cordonnier, C. Demuynck, J. L. Destombes and A. G. Csaszar, Milimiter– and Submilimiter–Wave Spectroscopy of Dibridged Si_2H_2 Isotopomers: Experimental and Theoretical Structure, *J. Chem. Phys.* **1994**, *100*, 8614–8624.
[19] X. Wang, L. Andrews and G. P. Kushto, Infrared Spectra of the Novel Ge_2H_2 and Ge_2H_4 and the Reactive $GeH_{1,2,3}$ Intermediates in Solid Neon, Deuterium and Argon, *J. Phys. Chem. A* **2002**, *106*, 5809–5816.
[20] J. Moc and M. Wierzejewska, Isomerization Pathways of Singlet Ga_2H_2: Quantum–Mechanical Predictions, *Chem. Phys. Lett.* **2003**, *380*, 304–312.
[21] T. H. Dunning, Gaussian Basis Sets for Use in Correlated Molecular Calculations. I. The Atoms Boron through Neon and Hydrogen, *J. Chem. Phys.* **1989**, *90*, 1007–1023.
[22] R. A. Kendall, T. H. Dunning and R. J. Harrison, Electron Affinities of the First–Raw Atoms Revisited. Systematic Basis Sets and Wave Functions, *J. Chem. Phys.* **1992**, *96*, 6796–6806.
[23] D. E. Woon and T. H. Dunning, Gaussian Basis Sets for Use in Correlated Molecular Calculations. III. The Atoms Aluminum Through Argon, *J. Chem. Phys.* **1993**, *98*, 1358–1371.
[24] J. A. Pople, J. S. Binkley, R. Seeger, Theoretical Models Incorporating Electron Correlation, *Int. J. Quantum Chem. Symp.* **1976**, *10*, 1–19.
[25] K. Raghavachari, G. W. Trucks, J. A. Pople and M. Head–Gordon, A Fifth–Order Perturbation Comparison of Electron Correlation Theories, *Chem. Phys. Lett.* **1989**, *157*, 479–483.
[26] C. Gonzalez and H. B. Schlegel, An Improved Algorithm for Reaction Path Following, *J. Chem. Phys.* **1989**, *90*, 2154–2161.
[27] M. J. Frisch, G. W. Trucks, H. B. Schlegel, G. E. Scuseria, M. A. Robb, J. R. Cheeseman, V. G. Zakrzewski, J. A. Montgomery, Jr., R. E. Stratman, J. C. Burant, S. Dapprich, J. M. Millam, A. D. Daniels, K. N. Kudin, M. C. Strain, O. Farkas, J. Tomasi, V. Barone, M. Cossi, R. Cammi, B. Mennucci, C. Pomelli, C. Adamo, C. Clifford, J. Ochterski, G. A. Petersson, P. Y. Ayala, Q. Cui, K. Morokuma, D. K. Malick, A. D. Rabuck, K. Raghavachari, J. B. Foresman, J. Cioslowski, J. V. Ortiz, B. B. Stefanov, G. Liu, A. Liashenko, P. Piskorz, I. Komaromi, R. Gomperts, R. L. Martin, D. J. Fox, T. Keith, M. A. Al–Laham, C. Y. Peng, A. Nanayakkara, C. Gonzalez, M. Challacombe, P. M. W. Gill, B. Johnson, W. Chen, M. W. Wong, J. L. Andres, M. Head–Gordon, E. S. Repogle and J. A. Pople, *Gaussian 98*, *Revision A.1x*, Gaussian, Inc., Pittsburgh, PA, 2001.